

# PulmoVec: A Two-Stage Stacking Meta-Learning Architecture Built on the HeAR Foundation Model for Multi-Task Classification of Pediatric Respiratory Sounds

Izzet Turkalp Akbasli<sup>1,\*</sup> and Oguzhan Serin<sup>2,\*</sup>

<sup>1</sup>Department of Pediatric Intensive Care Medicine, Life Support Center, Hacettepe University, Ankara, Türkiye

<sup>2</sup>Department of Pediatric Emergency Medicine, Life Support Center, Hacettepe University Faculty of Medicine, Ankara, Türkiye

\* \* Indicates co-first authors

## Corresponding Author:

Izzet Turkalp Akbasli, MD

Department of Pediatric Emergency Medicine, Hacettepe University Faculty of Medicine  
06100 Sıhhiye, Ankara, Turkey

Email: [iakbasli@hacettepe.edu.tr](mailto:iakbasli@hacettepe.edu.tr)

Telephone: +90 312 305 1350

ORCID: 0000-0003-3055-7355

**Running Head:** PulmoVec for Pediatric Respiratory Sounds

**Keywords:** *pediatric respiratory sounds, lung sound classification, foundation audio model, HeAR, transfer learning, stacking ensemble, LightGBM, digital auscultation, SPRSound*

## Abstract

**Background:** Respiratory diseases are a leading cause of childhood morbidity and mortality, yet lung auscultation remains subjective and limited by inter-listener variability, particularly in pediatric populations. Existing AI approaches are further constrained by small datasets and single-task designs. We developed PulmoVec, a multi-task framework built on the Health Acoustic Representations (HeAR) foundation model for classification of pediatric respiratory sounds.

**Methods:** In this retrospective analysis of the SPRSound database, 24,808 event-level annotated segments from 1,652 pediatric patients were analyzed. Three task-specific classifiers were trained for screening, sound-pattern recognition, and disease-group prediction. Their out-of-fold probability outputs were combined with demographic metadata in a LightGBM stacking meta-model, and event-level predictions were aggregated to the patient level using ensemble voting.

**Results:** At the event level, the screening model achieved an ROC-AUC of 0.96 (95% CI, 0.95–0.97), the sound-pattern recognition model a macro ROC-AUC of 0.96 (95% CI, 0.96–0.97), and the disease-group prediction model a macro ROC-AUC of 0.94 (95% CI, 0.93–0.94). At the patient level, disease-group classification yielded an accuracy of 0.74 (95% CI, 0.71–0.77), a weighted F1-score of 0.73, and a macro ROC-AUC of 0.91 (95% CI, 0.90–0.93). Stacking improved performance across all tasks compared with base models alone.

**Conclusions:** PulmoVec links event-level acoustic phenotyping with patient-level clinical classification, supporting the potential of foundation-model-based digital auscultation in pediatric respiratory medicine. Multi-center external validation across devices and real-world conditions remains essential.

## INTRODUCTION

### Background and Motivation

Respiratory diseases are among the leading causes of morbidity and mortality in children worldwide, with lower respiratory tract infections continuing to represent a major cause of hospitalization and death, particularly in low and middle-income countries [1, 2]. Pneumonia, in particular, remains the major contributor to childhood mortality, accounting for 14% of all deaths in children under five years of age and causing 740,180 deaths in 2019; timely and accurate diagnosis has been shown to reduce mortality by up to 28% [1]. To support early and accurate diagnostic decision-making in children with respiratory disease, clinicians rely on lung auscultation, a clinical technique that involves identifying pathological patterns in respiratory sounds using a stethoscope and that has remained a fundamental skill for nearly two centuries [3, 4]. Despite its longstanding clinical use, lung auscultation remains inherently subjective, and substantial variability in the interpretation of respiratory sounds can occur even among trained clinicians [5]. These difficulties are further amplified in pediatric populations, where patient cooperation is limited and respiratory physiology differs from that of adults [6, 7]. Recent advances in digital stethoscopes and smartphone-based recording technologies now enable the acquisition, storage, and computational analysis of respiratory sounds, creating new opportunities for objective evaluation and automated diagnostic support [3, 8, 9].

### Problem Statement

The existing pediatric respiratory sound classification literature is characterized by notable limitations. Most studies rely on small, single-center datasets, and heterogeneity across recording devices, annotation protocols, and label taxonomies limits cross-study comparability [10, 11, 12]. Most current architectures employ single-task classifiers, which may not capture the full clinical complexity of respiratory sounds in children [3, 11]. In this context, the central research question is as follows: can a foundation audio model trained through large-scale self-supervised learning recognize acoustic patterns in pediatric respiratory sounds in a clinically meaningful way, and can a multi-task stacking architecture improve upon the performance of existing single-task approaches?

## Research Gap and Objectives

The recent emergence of self-supervised foundation audio models for health acoustics has opened new possibilities. One of the most influential is Health Acoustic Representations (HeAR), a large-scale foundation encoder trained on 313.3 million audio clips from roughly 3 billion YouTube videos, with demonstrated strength across multiple health acoustics tasks [13]. Despite this progress, most applications of HeAR rely on simple single-task classifiers, and research on multi-task stacking architectures for respiratory sound classification remains limited [14, 15]. Recent reviews further highlight persistent gaps in explainability, external validation, and clinically meaningful label design [3, 10, 11, 16].

To address these limitations, this study introduces PulmoVec, a two-stage architecture that leverages HeAR as a shared acoustic backbone and integrates three complementary task-specific base classifiers with a LightGBM stacking meta-model that incorporates demographic metadata. The system is designed to mirror a stepwise clinical decision-support workflow: first distinguishing normal from abnormal sounds, then identifying the specific sound pattern, followed by predicting the disease group associated with pathological patterns, and finally integrating acoustic outputs with clinical variables such as age, sex, and recording location to generate more clinically meaningful predictions.

## METHODS

### Study Design and Data Source

This study is based on a retrospective analysis of the publicly available SPRSound pediatric respiratory sound database, collected using an electronic stethoscope at Shanghai Children’s Medical Center (SCMC) [17]. SPRSound provides both record-level and event-level annotations (Normal, Fine Crackle, Coarse Crackle, Wheeze, Wheeze&Crackle, Rhonchi, Stridor) with millisecond-precision timestamps, generated by 11 experienced pediatric physicians [17]. The database encompasses 16 distinct disease diagnoses; the detailed distribution of these diagnoses is provided in the supplementary material (Supplementary Table S1). Because this study used a publicly available, pre-anonymized dataset and involved no direct participant contact or access to identifiable private information, additional institutional review board approval and individual informed consent were not required for the present secondary analysis. Study design, analysis, and reporting were conducted in accordance with TRIPOD+AI recommendations, and the completed TRIPOD+AI checklist is provided in Supplementary Appendix 1.

### Data Curation

Data curation was performed in three stages: (1) removal of potential duplicate recordings, (2) exclusion of recordings labeled as “Poor Quality” at the record level, and (3) exclusion of recordings lacking event-level annotations. There were no missing data in the final analytic dataset for the variables used in model development, including age, sex, recording location, and event-level labels; accordingly, no imputation procedures were performed. Segments labeled as “No Event” in event-level annotations were included in the Normal class, consistent

with their clinical interpretation. The current expanded version of the SPRSound database was used.

## Audio Preprocessing and Feature Extraction

All signals were resampled to 16 kHz mono and standardized to 2.0-second windows (zero-padded if shorter, center-cropped if longer). A 10% overlap margin was applied around event boundaries. Acoustic feature extraction was performed using the HeAR foundation audio model [13], producing a 512-dimensional embedding vector for each clip.

## Base Classifier Architecture and Label Design

Three task-specific base classifiers were constructed on the shared HeAR embedding space. The classification head architecture was identical across all models: a fully connected layer (512 to 256 neurons), nonlinear activation, dropout ( $p = 0.3$ ), and an output layer. The Sound Pattern Recognition Model classified events as Normal, Crackles (combining Fine and Coarse Crackle), or Rhonchi (wheeze and rhonchi-like continuous patterns). The Screening Model performed a Normal/Abnormal distinction. The Disease Group Prediction Model mapped the 16 disease labels in SPRSound to four clinically meaningful groups: Pneumonia (severe and non-severe), Bronchial diseases (asthma, bronchitis, bronchiolitis, bronchiectasis, and protracted bacterial bronchitis), Normal (control group), and Others (upper respiratory tract infection, hemoptysis, pulmonary hemosiderosis, chronic cough, airway foreign body, Kawasaki disease, and other respiratory diseases). The complete label mapping from original annotations to study targets is provided in Supplementary Table S2.

## Two-Stage Fine-Tuning Protocol

Training followed a two-stage protocol. In the first stage, the HeAR encoder was frozen and only the classification head was optimized for 10 epochs at a learning rate of  $1 \times 10^{-4}$ . In the second stage, the encoder was unfrozen and the entire model was fine-tuned for 40 epochs at a learning rate of  $5 \times 10^{-7}$ . Class imbalance was addressed through class weighting in the loss function, and early stopping based on validation performance was applied.

## Stacking Meta-Learning

After training the base models, an out-of-fold approach was used to prevent data leakage from base model predictions into the meta-model training data: probability outputs for each training example were generated using a fold in which that example was not part of the training set. A total of 9 probability-based features were obtained from the three base models (3 from the Sound Pattern Recognition Model, 2 from the Screening Model, and 4 from the Disease Group Prediction Model). These probability features were combined with age, sex, and recording location to form an 11-dimensional meta-feature matrix. Three clinical classification targets are presented in this study: Screening (Normal/Abnormal), Sound Pattern (Normal/Crackles/Rhonchi), and Disease Group (Pneumonia/Bronchial Diseases/Normal/Others). LightGBM hyperparameters were independently optimized for each

target using Optuna-based Bayesian search. Training hyperparameters and LightGBM optimization search ranges are detailed in Supplementary Table S4. Results for additional classification targets (including a 7-class event type and a 16-disease detailed model) are provided in the supplementary material (Supplementary Table S3; Supplementary Figures S2 and S3).

## Patient-Level Aggregation: Ensemble Voting

Since clinical decision-making occurs at the patient level, an ensemble voting method combining three complementary strategies was developed to aggregate event-level predictions to the patient level: simple soft voting (weight: 30%), confidence-weighted voting (weight: 40%), and majority voting (weight: 30%). Majority voting was activated only when at least 60% of events agreed on a class and at least 50% showed high confidence ( $> 0.7$ ); otherwise, the system fell back to soft voting. The final patient-level prediction was calculated as a weighted linear combination of the three strategies. The relative weights were determined empirically using the validation set through a predefined search over candidate combinations, prioritizing stable patient-level decisions and balanced class performance rather than overall accuracy alone.

The weights and decision thresholds in this ensemble scheme were not chosen arbitrarily but were selected by jointly evaluating performance and decision stability on the validation split. Different weight combinations were tested in a predefined search, with selection based not only on overall accuracy but also on maintaining balance across classes, reducing excessive volatility in low-sample classes, and preventing a single high-probability segment from disproportionately driving the patient-level decision. Similarly, the  $> 0.7$  probability threshold was set to ensure that only consistently dominant patterns generated patient-level decisions. These parameters should be viewed not as universal optima but as empirical design parameters that yielded the most balanced validation performance under the noise structure and class distribution of the current dataset.

## Codebase, Model Evaluation, and Accessibility

Performance was evaluated using accuracy, weighted-F1, macro-F1, per-class precision, recall, specificity, NPV, ROC-AUC, and Precision-Recall analysis. In multi-class tasks, ROC-AUC values were computed using the one-vs-rest approach and reported as macro averages. The overall adequacy of probabilistic outputs was summarized using the Brier score. 95% confidence intervals were computed using nonparametric bootstrap with 1,000 iterations at the patient level in the test set. All analyses were conducted using Python 3.11.2, with pandas, NumPy, PyTorch, scikit-learn, and SciPy libraries. Processed data, code, and explanatory documentation are provided in a publicly available GitHub repository to support reproducibility (<https://github.com/turkalpmd/PulmoVec>).

# RESULTS

## Cohort Characteristics

The final analysis cohort after curation consisted of 1,652 unique patients and 24,808 event-level labeled sound segments. Stratified patient-level splitting allocated 1,321 patients (20,567 events) to the training set and 331 patients (4,241 events) to the test set. No statistically significant differences were observed between the two groups in terms of age ( $p = 0.066$ ), disease group distribution ( $p = 1.000$ ), sound pattern distribution ( $p = 0.181$ ), or recording location ( $p = 0.307$ ) (Table 1). The cohort comprised 54.7% pneumonia, 21.8% bronchial diseases, 9.7% control group, and 13.9% other respiratory diseases (see Supplementary Table S1 for the detailed 16-disease distribution).

Table 1: *Cohort descriptive statistics. Categorical variables: chi-square test; continuous variables: Mann-Whitney U test. \*No Event segments were included in the Normal class.*

Variable	All Cohort (n)	Train n (%)	Test n (%)	p value
<b>Total patients</b>	1,652	1,321	331	—
<b>Sex</b>				0.105
Male	850	666 (50.4)	184 (55.6)	
Female	802	655 (49.6)	147 (44.4)	
<b>Age (years), median (IQR)</b>	—	5.0 (3.4–7.4)	4.5 (3.3–7.0)	0.066
<b>Disease group (patient-level)</b>				1.000
Pneumonia	904	723 (54.7)	181 (54.7)	
Bronchial diseases	359	287 (21.7)	72 (21.8)	
Normal	159	127 (9.6)	32 (9.7)	
Others	230	184 (13.9)	46 (13.9)	
<b>Total events</b>	24,808	20,567	4,241	—
<b>Event type distribution</b>				0.181
Normal	18,772	15,623 (76.0)	3,149 (74.3)	
Fine Crackle	3,530	2,909 (14.1)	621 (14.6)	
Coarse Crackle	177	161 (0.8)	16 (0.4)	
Wheeze	1,505	1,254 (6.1)	251 (5.9)	
Wheeze+Crackle	303	229 (1.1)	74 (1.7)	
Rhonchi	217	201 (1.0)	16 (0.4)	
Stridor	74	18 (0.1)	56 (1.3)	
No Event*	230	172 (0.8)	58 (1.4)	
<b>Sound pattern distribution</b>				0.181
Normal	19,002	15,795 (76.8)	3,207 (75.6)	
Crackles	4,010	3,299 (16.0)	711 (16.8)	
Rhonchi	1,796	1,473 (7.2)	323 (7.6)	
<b>Recording location (p1–p4)</b>				0.307
p1	6,243	5,162 (25.1)	1,081 (25.5)	
p2	6,555	5,400 (26.3)	1,155 (27.2)	
p3	5,765	4,814 (23.4)	951 (22.4)	
p4	6,038	5,030 (24.5)	1,008 (23.8)	

## Event-Level Classification

When comparing individual HeAR base model outputs with the final LightGBM stacking meta-model outputs at the event level, performance gains of 9 to 12 percentage points were observed across all tasks. For the first two event-level acoustic segment classification models, performance metrics were as follows: the Screening Model achieved an accuracy of 0.92 (95% CI, 0.92 to 0.93), weighted-F1 of 0.92, and ROC-AUC of 0.96 (95% CI, 0.95 to 0.97), with a Brier score of 0.12 (95% CI, 0.11 to 0.13). The Sound Pattern Recognition Model achieved

an accuracy of 0.91 (95% CI, 0.90 to 0.92), weighted-F1 of 0.91, and macro ROC-AUC of 0.96 (95% CI, 0.96 to 0.97), with a Brier score of 0.14 (95% CI, 0.12 to 0.15). Per-class performance metrics for the Sound Pattern Recognition Model are presented in Table 2.

Table 2: *Sound Pattern Recognition Model per-class performance metrics.*

<b>Class</b>	<b>ROC-AUC (OvR)</b>	<b>F1-Score</b>	<b>Recall (Sensitivity)</b>	<b>Specificity</b>	<b>NPV</b>	<b>Precision (PPV)</b>
<b>Normal</b> ( $n = 3,743$ )	0.96 [0.95–0.96]	0.95 [0.94–0.95]	0.97 [0.96–0.97]	0.76 [0.74–0.79]	0.88 [0.86–0.89]	0.93 [0.92–0.94]
<b>Crackles</b> ( $n = 813$ )	0.95 [0.94–0.96]	0.74 [0.72–0.77]	0.68 [0.65–0.72]	0.97 [0.96–0.97]	0.94 [0.93–0.95]	0.82 [0.79–0.84]
<b>Rhonchi</b> ( $n = 345$ )	0.98 [0.97–0.99]	0.86 [0.83–0.88]	0.83 [0.80–0.87]	0.99 [0.99–0.99]	0.99 [0.98–0.99]	0.88 [0.84–0.91]

Values are reported with 95% confidence intervals. ROC-AUC = area under the receiver operating characteristic curve; F1-score = harmonic mean of precision and recall; Recall = sensitivity; Specificity = true negative rate; PPV = positive predictive value; NPV = negative predictive value.

**Model 1: Event Type Classification - Event Type: Crackles**

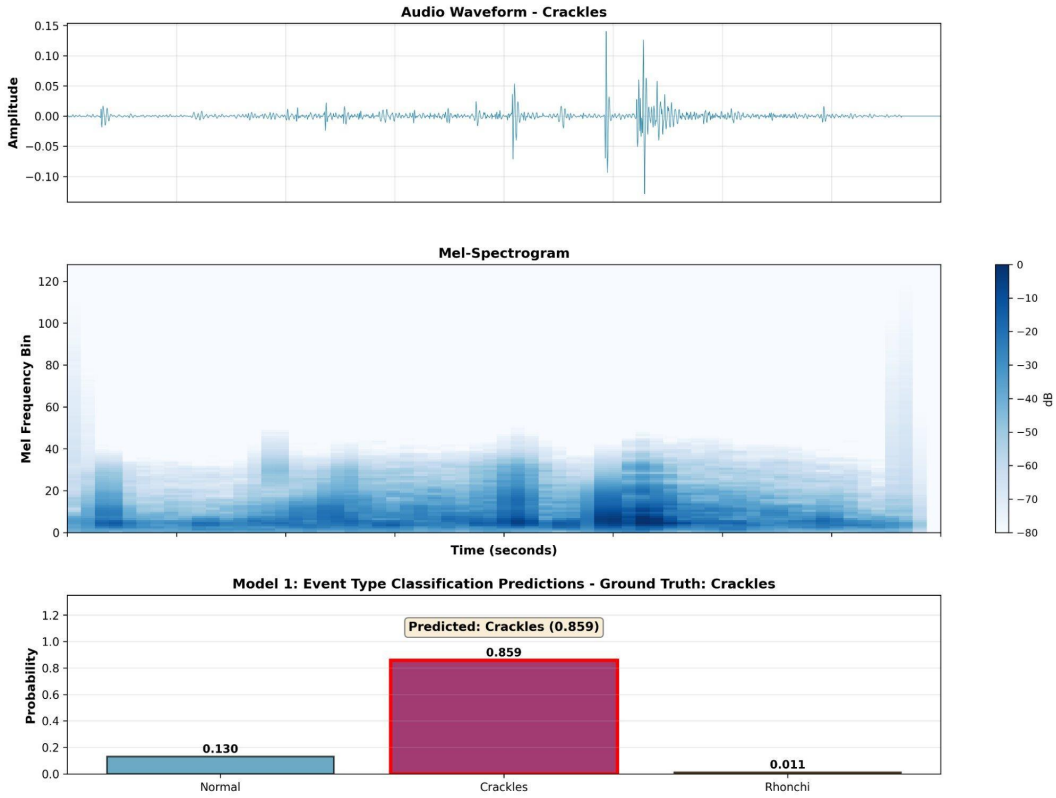


Figure 1: *Qualitative performance example for a segment annotated as Crackles: Example qualitative prediction for a respiratory sound segment labeled as crackles. The top panel shows the raw audio waveform, the middle panel displays the corresponding Mel-spectrogram representation, and the bottom panel presents the model’s predicted class probabilities for Normal, Crackles, and Rhonchi. The model correctly identifies the segment as crackles with high confidence (0.859).*

The Disease Group Prediction Model achieved an accuracy of 0.80 (95% CI, 0.78 to 0.81), weighted-F1 of 0.79, and macro ROC-AUC of 0.94 (95% CI, 0.93 to 0.94), with a Brier score of 0.29 (95% CI, 0.28 to 0.31). Per-class results are shown in Table 3. Event-level confusion matrices for all classification tasks are provided in Supplementary Figure S2.

Table 3: *Disease Group Prediction Model event-level per-class performance metrics.*

<b>Class</b>	<b>ROC-AUC (OvR)</b>	<b>F1-Score</b>	<b>Recall (Sensitivity)</b>	<b>Specificity</b>	<b>NPV</b>	<b>Precision (PPV)</b>
<b>Pneumonia</b> ( <i>n</i> = 2,436)	0.93 [0.92–0.94]	0.85 [0.84–0.86]	0.89 [0.88–0.90]	0.81 [0.79–0.82]	0.88 [0.87–0.89]	0.82 [0.81–0.84]
<b>Bronchial diseases</b> ( <i>n</i> = 920)	0.92 [0.91–0.93]	0.68 [0.66–0.70]	0.63 [0.59–0.66]	0.95 [0.94–0.96]	0.92 [0.91–0.93]	0.75 [0.72–0.78]
<b>Normal</b> ( <i>n</i> = 405)	0.94 [0.93–0.95]	0.61 [0.57–0.65]	0.54 [0.49–0.59]	0.98 [0.98–0.98]	0.96 [0.95–0.97]	0.71 [0.66–0.76]
<b>Others</b> ( <i>n</i> = 1,140)	0.96 [0.96–0.97]	0.81 [0.79–0.82]	0.82 [0.80–0.84]	0.94 [0.93–0.94]	0.95 [0.94–0.95]	0.79 [0.77–0.82]

Values are reported with 95% confidence intervals. ROC-AUC = area under the receiver operating characteristic curve; F1-score = harmonic mean of precision and recall; Recall = sensitivity; Specificity = true negative rate; PPV = positive predictive value; NPV = negative predictive value.

## Patient-Level Classification

Patient-level Disease Group Prediction Model results obtained through ensemble voting are presented in Table 4. At the patient level, accuracy was 0.74 (0.71 to 0.77), weighted-F1 was 0.73, and macro ROC-AUC was 0.91 (0.90 to 0.93). Compared to the event level, accuracy decreased by 0.06 points while macro ROC-AUC declined from 0.94 to 0.91. Patient-level recall for pneumonia (0.85) remained close to the event-level value (0.89); the Normal class had the lowest recall (0.39), and possible explanations for this finding are addressed in the Discussion. The patient-level Brier score was 0.35 (0.32 to 0.39). Patient-level ROC and Precision-Recall curves are shown in Figure 2.

Table 4: *Disease Group Prediction Model patient-level (ensemble voting) per-class performance metrics.*

Class	ROC-AUC (OvR)	F1-Score	Recall (Sensitivity)	Specificity	NPV	Precision (PPV)
<b>Pneumonia</b> ( $n = 386$ )	0.89 [0.86–0.91]	0.80 [0.78–0.83]	0.85 [0.81–0.88]	0.73 [0.68–0.77]	0.82 [0.77–0.86]	0.77 [0.73–0.81]
<b>Bronchial diseases</b> ( $n = 165$ )	0.91 [0.89–0.93]	0.64 [0.58–0.71]	0.58 [0.51–0.66]	0.94 [0.92–0.96]	0.89 [0.87–0.91]	0.72 [0.64–0.79]
<b>Normal</b> ( $n = 67$ )	0.92 [0.89–0.95]	0.48 [0.36–0.60]	0.39 [0.27–0.51]	0.98 [0.97–0.99]	0.94 [0.92–0.96]	0.65 [0.49–0.81]
<b>Others</b> ( $n = 134$ )	0.93 [0.91–0.96]	0.73 [0.67–0.78]	0.78 [0.71–0.85]	0.92 [0.90–0.94]	0.95 [0.93–0.97]	0.68 [0.61–0.75]

Values are reported with 95% confidence intervals. ROC-AUC = area under the receiver operating characteristic curve; F1-score = harmonic mean of precision and recall; Recall = sensitivity; Specificity = true negative rate; PPV = positive predictive value; NPV = negative predictive value.

**Patient-Level Disease Category (Ensemble Voting) - Multi-Class Performance Curves (Macro AUC = 0.913, Macro AP = 0.763)**

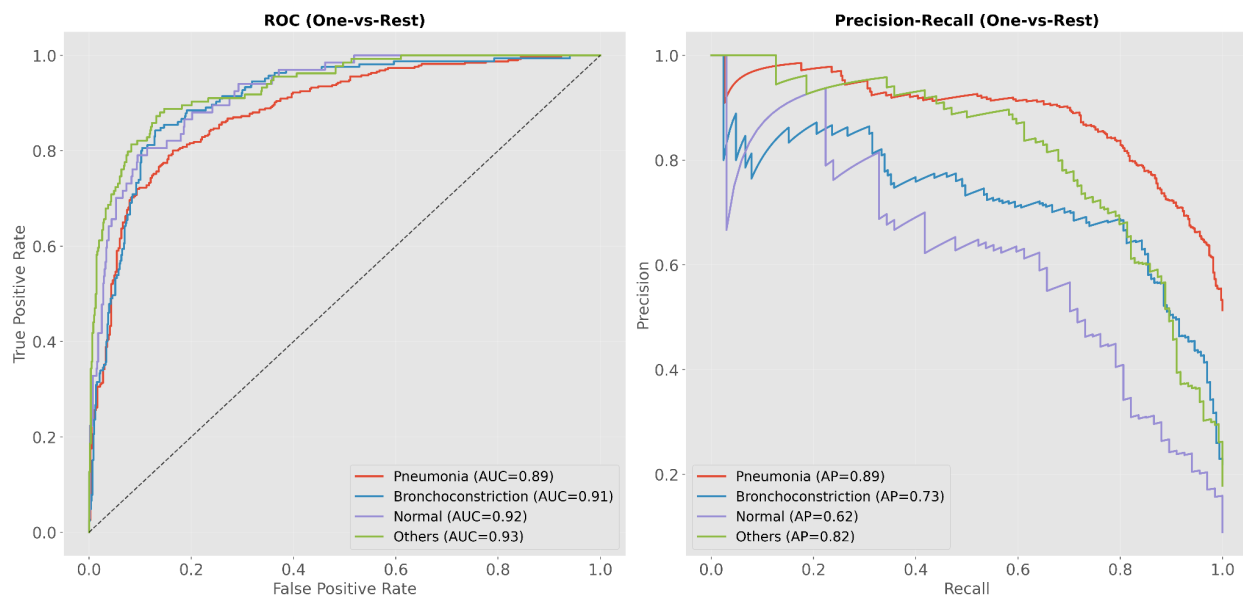


Figure 2: *Disease Group Prediction Model patient-level ROC and Precision-Recall curves (macro AUC=0.91; macro AUPRC=0.76).*

# DISCUSSION

The primary contribution of this study is the presentation of a multi-task, two-stage architecture that links event-level acoustic phenotyping to patient-level clinical decisions in pediatric respiratory sounds. PulmoVec combined the acoustic representations produced by the HeAR foundation model with base learners that classify from different clinical perspectives and modeled a stepwise decision process by incorporating demographic context through a stacking meta-learner. This approach differs structurally from the dominant single-task CNN paradigm in the literature and offers the ability to integrate clinical information at multiple levels.

## Strengths of the Study

PulmoVec is among the pediatric respiratory sound studies that combine the HeAR foundation model with a multi-task stacking architecture. Through probability-based feature fusion, the architecture transfers classification uncertainty to the meta-learner rather than losing it at the hard label level, which may allow for better representation of intermediate states among acoustic patterns. The ensemble voting strategy developed for transitioning from event-level predictions to patient-level decisions provides direct evaluation at the patient level, the natural unit of clinical decision-making. Probability calibration was quantified using Brier scores, and the observed values (0.12 to 0.29 at the event level; 0.35 at the patient level) suggest non-random probabilistic discrimination that varies across tasks, although class-specific reliability analyses and calibration curves would be valuable for a more comprehensive evaluation in the future. The use of the expanded version of SPRSound (1,652 patients, 24,808 events) constitutes one of the largest single-center studies in the pediatric respiratory sound domain.

## Comparison with the Literature

The meta-analysis by Park et al., covering 41 pediatric studies, reported pooled sensitivities of 0.90 for wheeze detection and 0.91 for abnormal sound detection [11]. The systematic review by Landry et al., encompassing 81 studies, reported classification accuracies in the 60 to 100% range while identifying substantial heterogeneity [10]. The patient-level macro ROC-AUC of 0.91 for PulmoVec’s Disease Group Prediction Model is broadly consistent with these meta-analytic estimates. The DeepBreath study reported an internal validation AUROC of 0.93 in 572 pediatric patients across five countries, but this value declined to 0.74 to 0.89 during external validation; this decline is a notable example underscoring the importance of the lack of external validation in the present study. In the multi-center wireless stethoscope trial, sensitivity and specificity exceeded 92% in subject-dependent scenarios [18, 19].

The recent pediatric lung sound AI literature shows that while performance metrics are promising, there is marked heterogeneity in datasets, labeling schemes, recording devices, and validation strategies [11]. Reviews evaluating the broader respiratory acoustics literature report that external validation, explainability, standardized label ontologies, and cross-device generalizability remain the main open issues in the field [10, 18]. In this context, the present

findings provide a strong internal validation signal, but the ultimate clinical value will become clear through multi-center external validation studies.

## Mechanism of the Stacking Architecture

The consistent performance gains observed across all tasks (9 to 12 percentage points in accuracy) likely effects not merely combining multiple model outputs, but to preserving and transferring probabilistic uncertainty to the meta-learner. By integrating demographic meta-data alongside base-model probabilities, the stacking architecture allows acoustic predictions to be interpreted within clinical context. Compared with hard label-level decision fusion, this approach may better capture intermediate states across acoustic patterns. The largest gains were observed in multi-class tasks, suggesting that the integration of complementary task-specific classifiers improved generalization in more complex prediction settings. The LightGBM-based meta-learner also enables examination of decision contributions through feature-importance rankings, providing a more interpretable framework than a fully opaque combination scheme [16, 20, 21].

## Transition from Event Level to Patient Level

In the Disease Group Prediction Model, accuracy decreased from 0.80 to 0.74 and macro ROC-AUC declined from 0.94 to 0.91 in the transition from event level to patient level. This decline is an expected finding in focal lung pathologies, where only the affected regions among multiple recording locations for a given patient produce pathological sounds. The preservation of patient-level recall for pneumonia (0.85) close to the event-level value (0.89) suggests that the ensemble voting strategy limited information loss in this class.

The relatively low recall observed for the Normal class at the patient level (0.39) should be interpreted not as a failure of the model to distinguish normal lung sounds, but as a reflection of the phase- and region-dependent nature of respiratory sounds. The classical auscultation literature describes wheezes as musical, predominantly expiratory sounds associated with airway obstruction, while crackles are short-duration, discontinuous sounds that are most prominent during the inspiratory phase [4, 22, 23]. Therefore, it is expected that some segments may appear acoustically normal even in patients with a diagnosis of bronchial diseases or pneumonia: while wheezes may be heard during both inspiration and expiration as obstruction severity increases, expiratory predominance is the classic pattern; crackles need not be present throughout the entire respiratory cycle [3, 7]. Such segmental heterogeneity can weaken the concordance between the patient-level label and the acoustic appearance at the short-window level, thereby reducing sensitivity particularly in the Normal class. This finding points not only to a model limitation but also to the inherently high intra-patient heterogeneity of pediatric respiratory sounds, suggesting that future respiratory cycle-aligned or inspiratory/expiratory phase-aware modeling strategies could improve patient-level decision performance. The disease versus event type distribution heatmap (Supplementary Figure S1) further illustrates this acoustic heterogeneity, confirming that normal-sounding segments predominate across nearly all disease categories.

## Digital Auscultation and Remote Monitoring Potential

The pre-training of HeAR on large-scale heterogeneous audio data aims to produce representations that can handle acoustic variability across different recording sources and devices. According to the HeAR model card, downstream models trained with HeAR have been shown to generalize well to sounds recorded from previously unseen devices [13]. While this property is conceptually relevant for scenarios where respiratory sounds may be recorded outside conventional clinical environments, this hypothesis was not directly tested in the present study. Recent evidence suggests that smartphone-based sound recording tools can also be used for pediatric respiratory assessment; Jeong et al. demonstrated the feasibility of respiratory assessment outside healthcare facilities using a smartphone-based self-auscultation tool [8]. Dent et al. highlighted the remote monitoring potential of artificial intelligence in preschool wheeze management [9]. Tzeng et al. showed that audio enhancement preprocessing improved classification robustness in noisy scenarios [24]. Taken together, these findings suggest that foundation model-based respiratory sound analysis may represent a promising avenue for digital auscultation-based decision support; however, its practical clinical value cannot be established until generalizability across devices, environments, and centers is systematically evaluated. Accordingly, future validation studies incorporating different recording devices and home-environment data will be essential to empirically assess this potential.

The clinical value of AI-assisted lung sound analysis will be determined not only by high discriminative performance but also by the ability to function reliably across different populations, devices, and care settings. The decline in performance observed in external cohorts in the DeepBreath study, despite strong internal validation, demonstrates that generalizability should be treated as a separate success criterion in pediatric lung sound models [18]. Accordingly, while the present results should be interpreted as a strong proof-of-concept for digital auscultation-based decision support, claims of clinical applicability will require confirmation through prospective, multi-center, and cross-device validation studies [11].

## Limitations

The most important limitation of this study is the absence of external validation. SPRSound originates from a single pediatric center and all recordings were obtained with the same electronic stethoscope model; as demonstrated by the DeepBreath study, external validation performance can decline substantially when geographic and device boundaries are crossed [18], and Yang et al. proposed a device-invariant framework specifically to address this issue [25]. While the patient-level aggregation strategy uses confidence-based weighting, it does not model temporal patterns or spatial relationships across locations; when considered alongside the low recall observed in the Normal class, this leaves room for improvement in the aggregation method. Class imbalance is particularly pronounced for rare disease labels, and the effect of additional balancing strategies beyond weighting (oversampling, augmentation, focal loss) was not systematically compared. Noise robustness was not directly tested with recordings from non-clinical environments, and annotation noise should be considered as a natural limitation of expert-labeled audio datasets.

## Future Directions

Multi-center external validation, ideally with prospective data collection across diverse devices and populations, is the most critical next step. Patient-level aggregation strategies that model temporal and spatial patterns, noise robustness assessment using synthetic noise injection and real-world home recordings, and prospective clinical utility studies are the priority directions for future research.

## Conclusion

PulmoVec shows that HeAR-based acoustic embeddings, multi-task classification, and patient-level aggregation can be combined into a clinically oriented framework for pediatric respiratory sound analysis. The findings support the feasibility of foundation-model-based digital auscultation for decision support, while underscoring the need for prospective multi-center and cross-device validation before clinical deployment.

## DECLARATIONS

**Acknowledgements:** None.

**Funding:** This research received no specific grant from any funding agency in the public, commercial, or not-for-profit sectors.

**Competing Interests:** The authors have no relevant financial or non-financial competing interests to disclose.

**Author Contributions:** I.T.A. led the conceptualization and methodology, developed the software, performed the formal analysis, curated the data, created the visualizations, wrote the original draft, and led project administration. O.S. contributed to validation, supervision, and writing–review & editing.

**Data Availability:** The datasets generated and analysed during the current study are publicly available in the Mendeley Data repository.

**Code Availability:** The custom code used in this study is available at <https://github.com/turkalpmd/PulmoVec>.

**Ethics Approval:** This study used retrospective, fully de-identified, publicly available data and was therefore exempt from institutional review board review and conducted in accordance with applicable ethical standards.

**Consent to Participate:** Informed consent was waived due to the retrospective use of fully de-identified data and minimal risk to patients.

**Consent to Publish:** Not applicable.

**Use of Generative Artificial Intelligence:** Generative artificial intelligence (*Claude Opus 4.6*) was used solely for language editing and clarity. No artificial intelligence was used in the generation of scientific content, data analysis, or interpretation. All authors reviewed and approved the final manuscript and take responsibility for its content.

## References

- [1] Serin O, Akbasli IT, Cetin SB, Koseoglu B, Deveci AF, Ugur MZ, Ozsurekci Y. Predicting Escalation of Care for Childhood Pneumonia Using Machine Learning: Retrospective Analysis and Model Development. *JMIRx Med* 2025;6(1):e57719.
- [2] Vos T, Lim SS, Abbafati C, Abbas KM, Abbasi M, et al. Global burden of 369 diseases and injuries in 204 countries and territories, 1990–2019: a systematic analysis for the Global Burden of Disease Study 2019. *The Lancet* 2020;396(10258):1204–1222.
- [3] Huang D-M, Huang J, Qiao K, Zhong N-S, Lu H-Z, Wang W-J. Deep learning-based lung sound analysis for intelligent stethoscope. *Mil Med Res* 2023;10(1):44.
- [4] Bohadana A, Izbicki G, Kraman SS. Fundamentals of Lung Auscultation. *N Engl J Med* 2014;370(8):744–751.
- [5] Aviles-Solis JC, Storvoll I, Vanbelle S, Melbye H. The use of spectrograms improves the classification of wheezes and crackles in an educational setting. *Sci Rep* 2020;10(1):8461.
- [6] Kotb MA, Elmahdy HN, Dein HMSE, Mostafa FZ, Refaey MA, Rjoob KQY, Draz IH, Basanti CWS. The Machine Learned Stethoscope Provides Accurate Operator Independent Diagnosis of Chest Disease. *Med Devices Evid Res* 2020;13:13–22.
- [7] Mor R, Kushnir I, Meyer J-J, Ekstein J, Ben-Dov I. Breath Sound Distribution Images of Patients With Pneumonia and Pleural Effusion. *Respir Care* 2007;52(12):1753–1760.
- [8] Jeong SG, Nam SW, Jung SK, Kim S-E. iMedic: Towards Smartphone-based Self-Auscultation Tool for AI-Powered Pediatric Respiratory Assessment. 2025. arXiv:2504.15743.
- [9] Dent A, Khan MK, Subbarao P. Leveraging artificial intelligence for the management of preschool wheeze: A narrative review. *Pediatr Allergy Immunol* 2025;36(10):e70207.
- [10] Landry V, Matschek J, Pang R, Munipalle M, Tan K, Boruff J, Li-Jessen NYK. Audio-based digital biomarkers in diagnosing and managing respiratory diseases: a systematic review and bibliometric analysis. *Eur Respir Rev* 2025;34(176):240246.
- [11] Park JS, Park S-Y, Moon JW, Kim K, Suh DI. Artificial Intelligence Models for Pediatric Lung Sound Analysis: Systematic Review and Meta-Analysis. *J Med Internet Res* 2025;27(1):e66491.
- [12] Moon HJ, Ji H, Kim BS, Kim BJ, Kim K. Machine learning-driven strategies for enhanced pediatric wheezing detection. *Front Pediatr* 2025;13. <https://doi.org/10.3389/fped.2025.1428862>
- [13] Baur S, Nabulsi Z, Weng W-H, Garrison J, Blankemeier L, Fishman S, Chen C, Kakarmath S, Maimbolwa M, Sanjase N, et al. HeAR — Health Acoustic Representations. 2024. arXiv:2403.02522.

- [14] Bauer MS, Damschroder L, Hagedorn H, Smith J, Kilbourne AM. An introduction to implementation science for the non-specialist. *BMC Psychol* 2015;3(1):32.
- [15] Ehtesham A, Kumar S, Singh A, Khoei TT. Pediatric Asthma Detection with Google’s HeAR Model: An AI-Driven Respiratory Sound Classifier. 2025. arXiv:2504.20124.
- [16] Kwong JCC, Khondker A, Lajkosz K, McDermott MBA, Frigola XB, McCradden MD, Mamdani M, Kulkarni GS, Johnson AEW. APPRAISE-AI Tool for Quantitative Evaluation of AI Studies for Clinical Decision Support. *JAMA Netw Open* 2023;6(9):e2335377.
- [17] Zhang Q, Zhang J, Yuan J, Huang H, Zhang Y, Zhang B, Lv G, Lin S, Wang N, Liu X, et al. SPRSound: Open-Source SJTU Paediatric Respiratory Sound Database. *IEEE Trans Biomed Circuits Syst* 2022;16(5):867–881.
- [18] Heitmann J, Glangetas A, Doenz J, Dervaux J, Shama DM, Garcia DH, Benissa MR, Cantais A, Perez A, Müller D, et al. DeepBreath—automated detection of respiratory pathology from lung auscultation in 572 pediatric outpatients across 5 countries. *Npj Digit Med* 2023;6(1):104.
- [19] Huang D, Wang L, Wang W. A Multi-Center Clinical Trial for Wireless Stethoscope-Based Diagnosis and Prognosis of Children Community-Acquired Pneumonia. *IEEE Trans Biomed Eng* 2023;70(7):2215–2226.
- [20] Sounderajah V, Ashrafian H, Rose S, Shah NH, Ghassemi M, Golub R, Kahn CE, Esteva A, Karthikesalingam A, Mateen B, et al. A quality assessment tool for artificial intelligence-centered diagnostic test accuracy studies: QUADAS-AI. *Nat Med* 2021;27(10):1663–1665.
- [21] Sounderajah V, Guni A, Liu X, Collins GS, Karthikesalingam A, Markar SR, Golub RM, Denniston AK, Shetty S, Moher D, et al. The STARD-AI reporting guideline for diagnostic accuracy studies using artificial intelligence. *Nat Med* 2025;31(10):3283–3289.
- [22] Reichenpfader D, Müller H, Denecke K. A scoping review of large language model based approaches for information extraction from radiology reports. *Npj Digit Med* 2024;7(1):1–12.
- [23] Sarkar M, Madabhavi I, Niranjana N, Dogra M. Auscultation of the respiratory system. *Ann Thorac Med* 2015;10(3):158.
- [24] Tzeng J-T, Li J-L, Chen H-Y, Huang C-H, Chen C-H, Fan C-Y, Huang EP-C, Lee C-C. Improving the Robustness and Clinical Applicability of Automatic Respiratory Sound Classification Using Deep Learning-Based Audio Enhancement: Algorithm Development and Validation. *JMIR AI* 2025;4(1):e67239.
- [25] Yang M, Liu X, Du W, Liu Y, Zhu W, Bu Z, Mao J, Wang Q, Chen S, Zhou M, et al. A device-invariant multi-modal learning framework for respiratory disease classification. *Npj Digit Med* 2026 Feb 26. <https://doi.org/10.1038/s41746-026-02445-4>

# Supplementary Material

*PulmoVec: A Two-Stage Stacking Meta-Learning Architecture Built on the HeAR Foundation Model for Multi-Task Classification of Pediatric Respiratory Sounds*  
Akbasli et al., 2026

Table S1: **Supplementary Table S1.** *Sixteen-Disease Distribution in the SPRSound Cohort. Full distribution of 16 disease diagnoses with train/test patient counts and event counts.*

Disease	Train patients	Test patients	Train events	Test events
Pneumonia (non-severe)	323	81	8,968	2,099
Unknown	94	26	3,793	1,020
Bronchitis	88	18	1,857	465
Control Group	55	19	1,615	429
Asthma	54	12	1,385	207
Pneumonia (severe)	30	11	966	305
Bronchiolitis	7	1	298	7
Other respiratory diseases	11	5	247	164
Bronchiectasis	5	3	202	114
Acute upper resp. infection	9	2	198	38
Hemoptysis	2	2	143	91
Chronic cough	4	0	55	0
Airway foreign body	2	0	38	0
Pulmonary hemosiderosis	1	1	32	40
Protracted bacterial bronchitis	1	0	21	0
Kawasaki disease	0	1	0	11

The SPRSound database contains 16 disease diagnoses spanning a broad spectrum of pediatric respiratory conditions. Pneumonia (severe and non-severe combined) accounts for the majority of both patients and events, followed by bronchitis and the control group. Several diagnoses, including Kawasaki disease, protracted bacterial bronchitis, and airway foreign body, are represented by very few patients, contributing to class imbalance in fine-grained classification tasks. The “Unknown” category includes patients for whom a definitive diagnosis could not be assigned from the available clinical records.

## **Supplementary Table S2.** *Label Mapping from Original Annotations to Study Targets*

The label mapping reflects two complementary design decisions. In Part A, the original seven adventitious event types were consolidated into three clinically actionable sound patterns: Normal, Crackles (combining fine and coarse crackle subtypes along with mixed wheeze-crackle events), and Rhonchi (grouping wheeze, stridor, and rhonchi as continuous obstructive patterns). No Event segments were treated as Normal in the Screening and Sound Pattern models. In Part B, the 16 original disease diagnoses were grouped into four syndrome-level categories guided by clinical reasoning: Pneumonia encompasses both

severity grades; Bronchial diseases includes conditions sharing obstructive airway physiology (asthma, bronchitis, bronchiolitis, bronchiectasis, and protracted bacterial bronchitis); Normal corresponds to the control group; and Others captures rarer and heterogeneous diagnoses where individual class sizes would be insufficient for reliable model training.

Table S2: **Part A.** *Event type to sound pattern mapping. \*No Event segments were included in the Normal class for the Sound Pattern Recognition Model and Screening Model.*

<b>Original event label</b>	<b>Sound pattern</b>
Normal	Normal
Fine Crackle	Crackles
Coarse Crackle	Crackles
Wheeze+Crackle	Crackles
Wheeze	Rhonchi
Stridor	Rhonchi
Rhonchi	Rhonchi
No Event	Normal*

Table S3: **Part B.** *Original diagnosis to four-class disease group mapping.*

<b>Original diagnosis</b>	<b>Disease group</b>
Pneumonia (severe)	Pneumonia
Pneumonia (non-severe)	Pneumonia
Asthma	Bronchial diseases
Bronchitis	Bronchial diseases
Bronchiolitis	Bronchial diseases
Bronchiectasis	Bronchial diseases
Protracted bacterial bronchitis	Bronchial diseases
Control Group	Normal
Acute upper resp. infection	Others
Airway foreign body	Others
Chronic cough	Others
Hemoptysis	Others
Kawasaki disease	Others
Other respiratory diseases	Others
Pulmonary hemosiderosis	Others
Unknown	Others

Table S4: **Supplementary Table S3.** *Additional Classification Results. Performance metrics for models not presented in the main manuscript. All metrics are from the stacking meta-model (LightGBM).*

Model	Classes	Accuracy	Macro F1	MCC	ROC-AUC (macro)
Event type (6-class)	Coarse Crackle, Fine Crackle, Normal, Rhonchi, Wheeze, Wheeze+Crackle	0.90 [0.89, 0.91]	0.67 [0.63, 0.71]	0.73 [0.71, 0.75]	0.97 [0.96, 0.97]
Disease (16-class)	All 16 diagnoses (see Table S1)	0.74 [0.73, 0.76]	0.60 [0.55, 0.65]	0.65 [0.62, 0.66]	0.98 [0.97, 0.98]

In addition to the three models presented in the main manuscript (Screening, Sound Pattern Recognition, and Disease Group Prediction), PulmoVec was also evaluated on two finer-grained classification targets. The 6-class event type model retained the original SPRSound adventitious sound taxonomy (excluding No Event and Stridor due to very low counts) and achieved a macro ROC-AUC of 0.97, indicating strong discriminative capacity even at high label granularity. The 16-class disease model attempted to predict the original diagnosis label directly, yielding a macro ROC-AUC of 0.98 despite a lower accuracy of 0.74, which reflects the challenge of hard classification under severe class imbalance while confirming that probability-based discrimination is largely preserved. These results were not included in the main manuscript to maintain focus on the three clinically grouped targets but are provided here for completeness.

Table S5: **Supplementary Table S4.** *Model Hyperparameters. Final hyperparameters for HeAR base models and LightGBM meta-model optimization ranges.*

Component	Parameter	Value
HeAR encoder	Model	google/hear-pytorch
HeAR encoder	Embedding dimension	512
Classification head	Hidden dimension	256
Classification head	Dropout	0.3
Training (Phase 1)	Epochs (frozen encoder)	10
Training (Phase 1)	Learning rate	$1 \times 10^{-4}$
Training (Phase 2)	Epochs (end-to-end)	40
Training (Phase 2)	Learning rate	$5 \times 10^{-7}$
Training	Batch size	32
LightGBM	n_estimators range	50–500 (Optuna)
LightGBM	max_depth range	3–15
LightGBM	learning_rate range	0.01–0.3 (log)
LightGBM	num_leaves range	15–300
LightGBM	min_child_samples range	5–100
LightGBM	subsample range	0.6–1.0
LightGBM	colsample_bytree range	0.6–1.0
LightGBM	early_stopping_rounds	20
LightGBM	Optimization	Optuna TPE, 100 trials

Training followed a two-stage fine-tuning protocol. In Phase 1, the HeAR encoder was frozen and only the classification head was trained at a higher learning rate to establish task-specific decision boundaries. In Phase 2, the full model including the encoder was fine-tuned at a substantially lower learning rate to adapt pretrained representations while minimizing catastrophic forgetting. LightGBM hyperparameters were optimized independently for each classification target using Optuna’s Tree-structured Parzen Estimator with 100 trials. The ranges listed above reflect the search space; final selected values varied across targets and are available in the code repository.

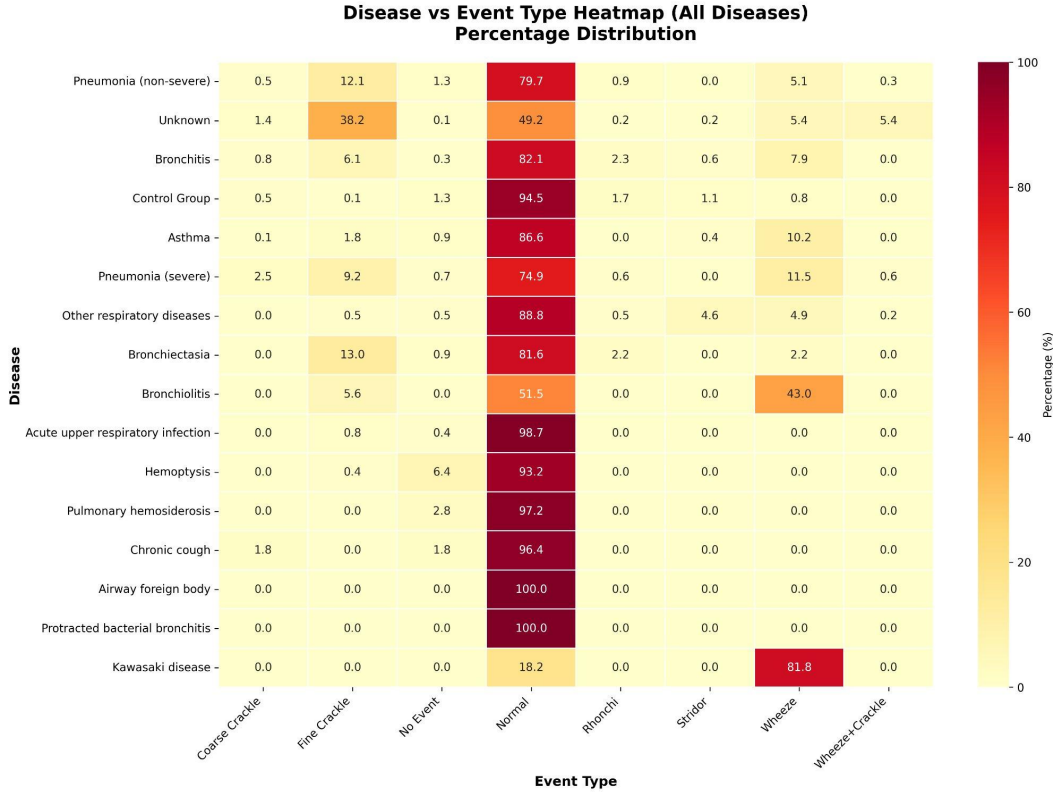
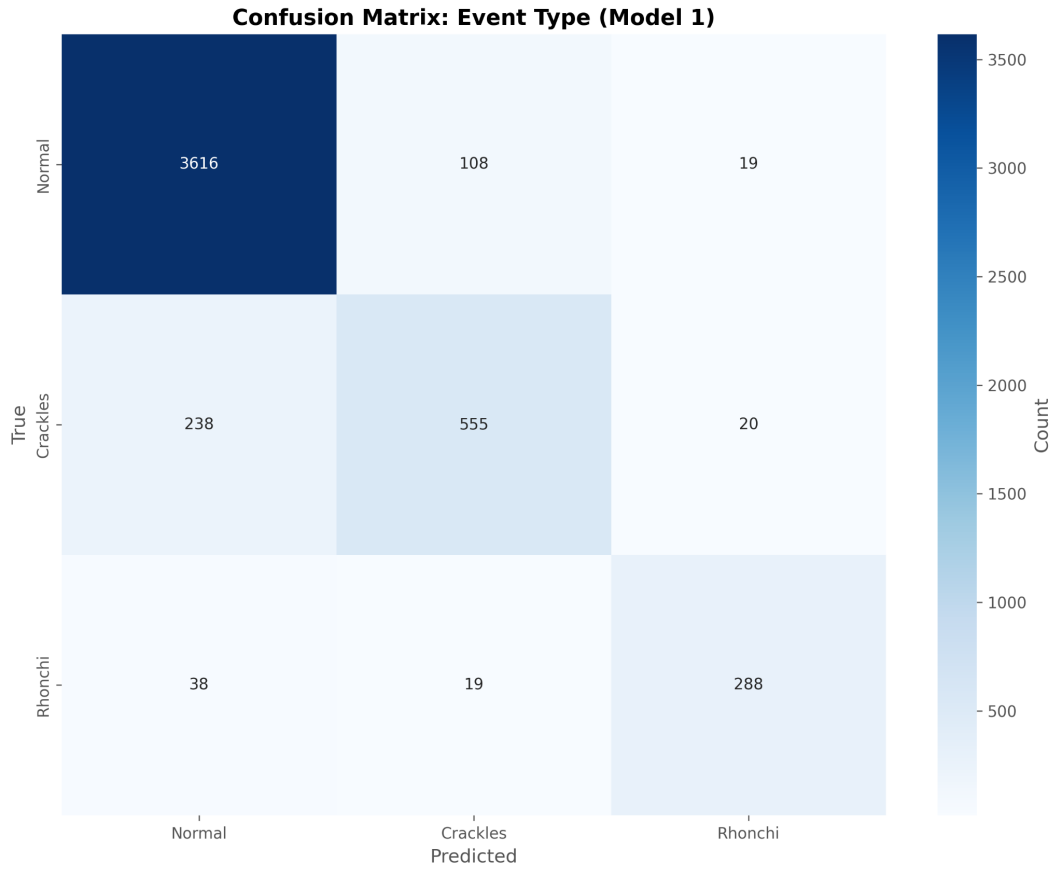


Figure S1: **Supplementary Figure S1.** *Disease versus event type heatmap.* Rows represent 16 disease diagnoses; columns represent 8 event types (including No Event). Cell values show the percentage distribution of event types within each disease.

This heatmap reveals several clinically relevant patterns. Normal-sounding segments dominate across nearly all diseases, consistent with the focal nature of most pediatric respiratory pathologies where only a fraction of recording locations and respiratory cycles produce adventitious sounds. Bronchiolitis shows the highest proportion of wheeze events (43%), reflecting its characteristic small airway obstruction. The Unknown category exhibits a uniquely high fine crackle prevalence (38%), suggesting that these patients may harbor undiagnosed parenchymal conditions. The control group shows 94.5% normal events, with the small proportion of adventitious sounds likely attributable to normal physiological variation and annotation sensitivity. Severe pneumonia shows more wheeze and coarse crackle events compared to non-severe pneumonia, consistent with greater inflammatory burden and airway involvement.

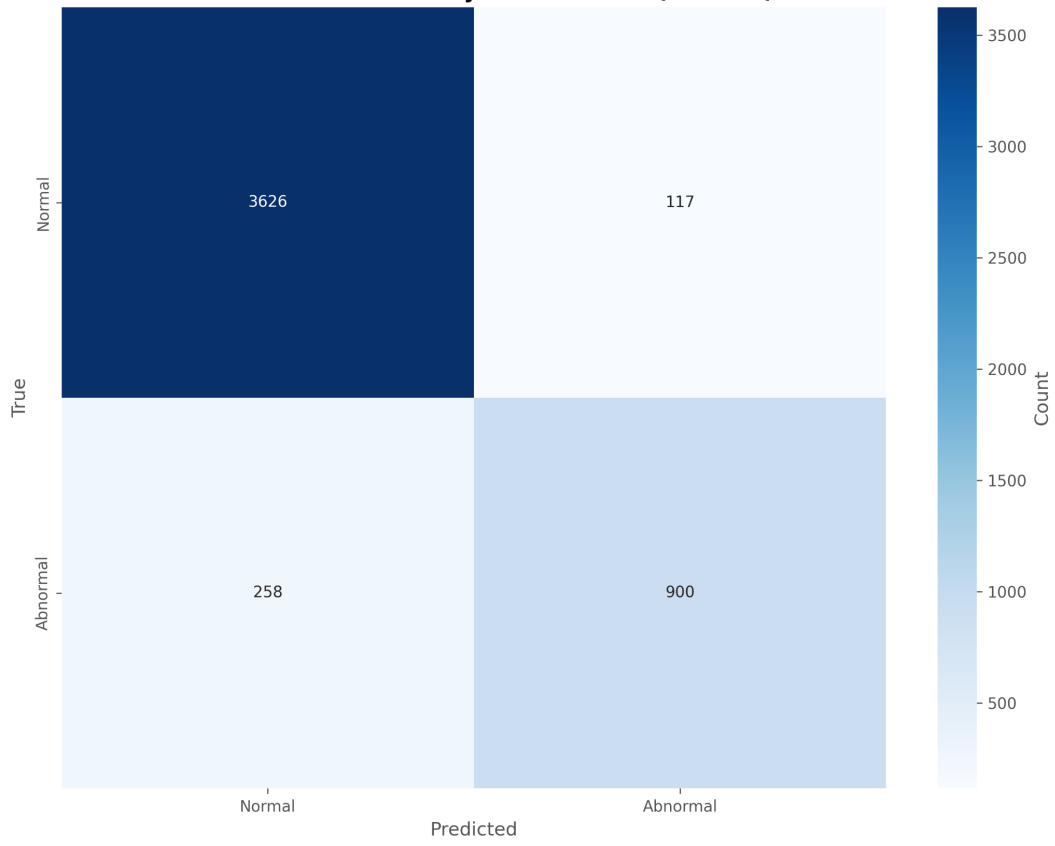
**Supplementary Figure S2.** *Confusion matrices for event-level classification tasks. (A) Sound Pattern Recognition Model (3-class). (B) Screening Model (2-class). (C) Event type model (6-class). (D) Disease Group Prediction Model (4-class).*

**(A) Sound Pattern Recognition Model**

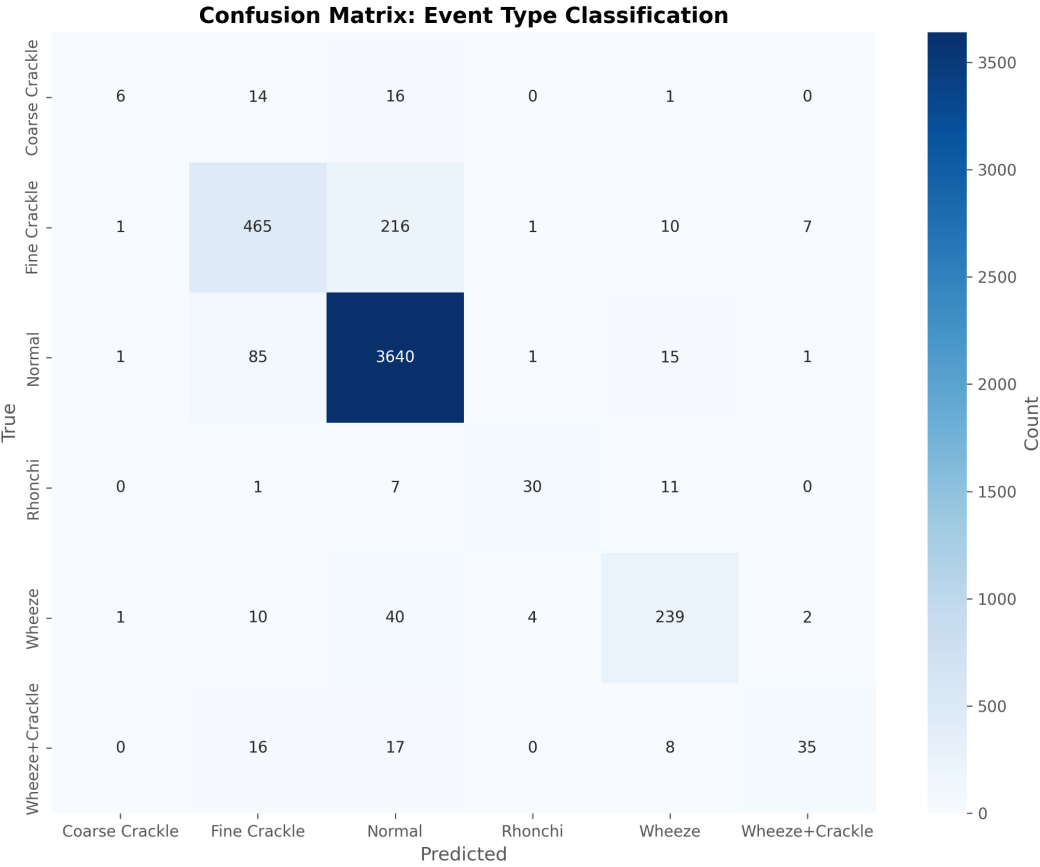


**(B) Screening Model**

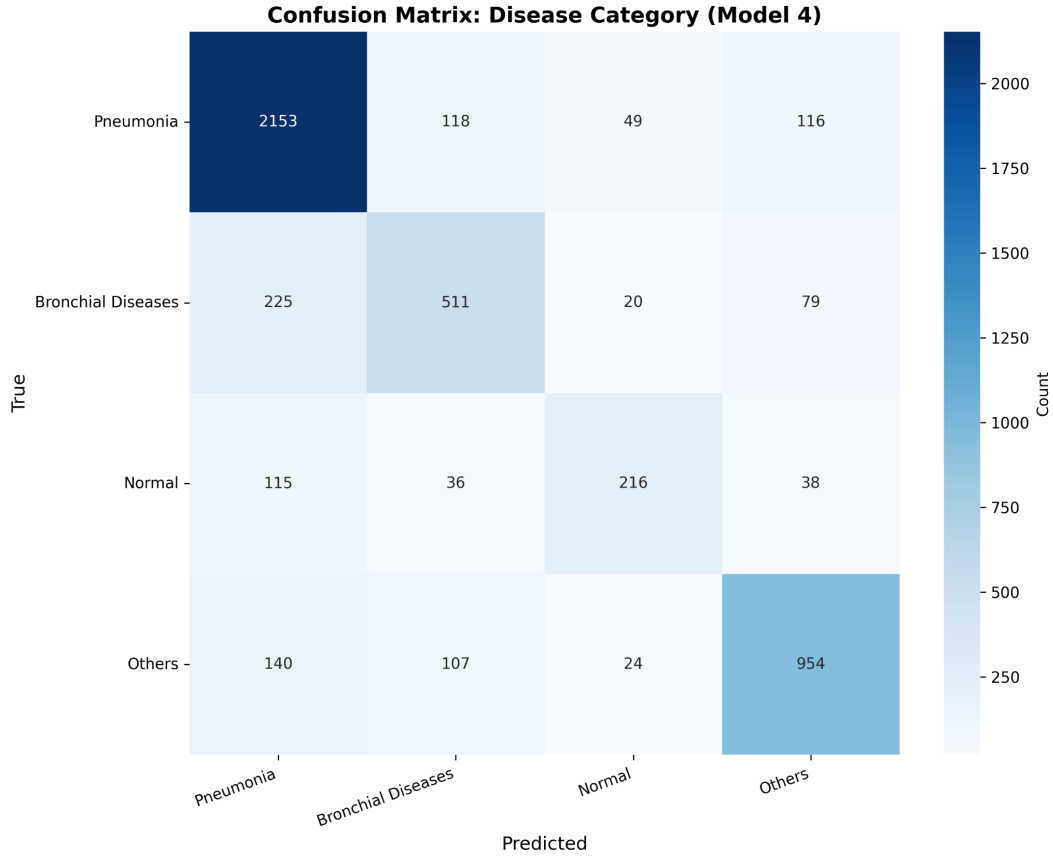
**Confusion Matrix: Binary Classification (Model 2)**



(C) Event Type Model (6-class)



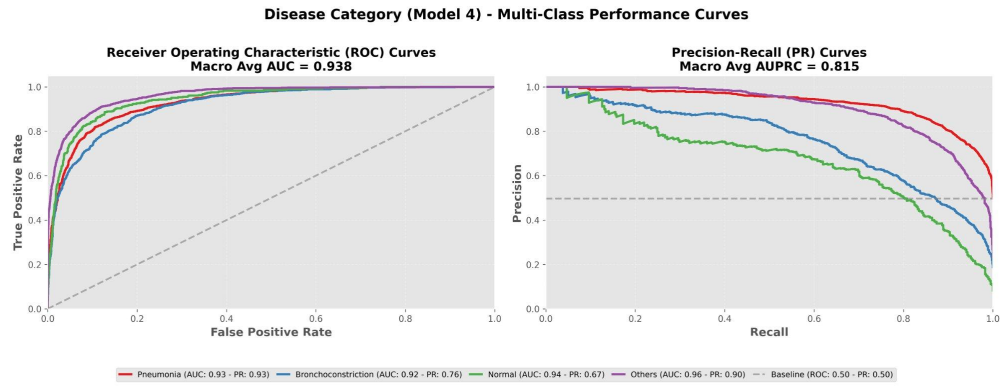
(D) Disease Group Prediction Model



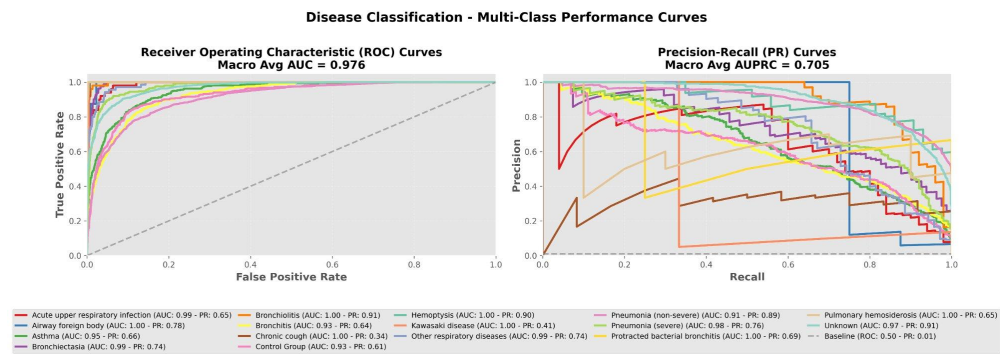
The confusion matrices illustrate the classification patterns across models of varying granularity. In the Sound Pattern Recognition Model (A), the primary confusion occurs between Normal and Crackles, with Rhonchi being well-separated. The Screening Model (B) shows high Normal recall (0.97) with some Abnormal events being misclassified as Normal, reflecting the challenge of detecting subtle adventitious sounds. The 6-class event type model (C) demonstrates that fine-grained event categories, particularly rare ones such as Coarse Crackle and Wheeze+Crackle, are more frequently confused with their dominant parent categories. The Disease Group Prediction Model (D) shows the strongest diagonal for Pneumonia, consistent with this class having the largest representation and the most distinct acoustic profile.

**Supplementary Figure S3.** ROC and Precision-Recall curves for additional models. (A) Disease Group Prediction Model (4-class, event level). (B) Disease model (16-class, event level).

**(A) Disease Group Prediction Model (4-class)**



**(B) Disease Model (16-class)**



The ROC curves demonstrate that probability-based discrimination remains strong even in the most granular classification scenario (16-class macro AUC = 0.98), despite the lower hard classification accuracy (0.74). This divergence between AUC and accuracy highlights that the model assigns higher probabilities to the correct class in most cases even when the argmax prediction is incorrect, suggesting that the probabilistic outputs carry clinically useful ranking information beyond the top-1 label. The Precision-Recall curves provide a complementary view that is more sensitive to class imbalance; the lower AUPRC values for rare classes confirm that prevalence-adjusted performance should be considered alongside standard ROC metrics when evaluating clinical utility for minority conditions.